Automotive Science and Engineering, Vol. 11, No. 3, (2021),3594-3613

Iran University of Science and Technology

Automotive Science and Engineering

Journal Homepage: ase.iust.ac.ir

ISSN: 2717-2023

Pareto optimization of a nonlinear vehicle model using multi-objective differential evolution algorithm with fuzzy inference-based adaptive mutation factor (MODE-FM)

M. Salehpour[1*], A. Bagheri[2]

[1] Department of Mechanical Engineering, Bandar Anzali Branch, Islamic Azad University, Bandar Anzali, Iran

[2] Faculty of Mechanical Engineering, University of Guilan, Rasht, Iran

ARTICLE INFO

Article history:

Received: 1 Aug 2021

Accepted:30 Aug 2021

Published:1 Sep 2021

Keywords:

Nonlinear vehicle vibration model

Pareto

Differential evolution

Multi-objective optimization

Road input

A B S T R A C T

In this study, a multi-objective differential evolution with fuzzy inference-based dynamic adaptable mutation factor with hybrid usage of non-dominated sorting and crowding distance (MODE-FM) is utilized for Pareto optimization of a 5-degree of freedom nonlinear vehicle vibration model considering the five conflicting functions simultaneously, under different road inputs. The significant conflicting objective functions that have been observed here are, namely, vertical seat acceleration, vertical forward tire velocity, vertical rear tire velocity, relative displacement between sprung mass and forward tire and relative displacement between sprung mass and rear tire. Different road inputs are, namely, double-bump, stationary random road and non-stationary random road. It is exhibited that the optimum solutions of 5-objective optimization contain those of 2-objective optimization and, as a result, this important matter creates more options for optimal design of nonlinear vehicle vibration model.

1. Introduction

Suspension system is a very important part of a vehicle which noticeably affects two significant criteria named ride comfort and road holding capability [1-2]. As a matter of fact, those aforesaid criteria are contradictory [3-4] and, of course, finding a proper compromise between them has always been a challenging task for researchers. Generally speaking, there exits three kinds of suspensions, namely, passive, semi-active and active ones [1-2, 5-6]. Passive suspensions are composed of parallel assembling of spring and damper between unsprung mass (vehicle wheel-axel) and sprung mass (vehicle body). In fact, passive suspensions can only obtain ride comfort or road holding capability, but, semi-active ones are capable of providing improvement because of their varying damping nature and low level of energy usage [1, 7]. Active suspensions need an additional energy supply for an actuator which is installed between sprung and unsprung masses [1, 5]. These types of suspensions are capable of achieving encouraging outcome in comparison with passive and semi-active ones [1]. The aforesaid confliction between ride comfort and road holding ability provide such a great necessity for finding trade-off between them. It can be readily observed that optimization methods are very helpful and applicable in this case.

As a matter of fact, optimization in engineering problems (such as vehicle suspension system design) has always had a significant role which leads towards producing several optimal methods. In this way, evolutionary algorithms (EAs) based on their intrinsic parallelism and stochastic nature are strongly useful and, as a result, have been widely used amongst all of the optimization approaches. On the other hand, the aforesaid

*M. Salehpour
Email Address: farbod.salehpour@gmail.com
https://doi.org/10.22068/ase.2021.595

[DOI: 10.22068/ase.2021.595]

characteristics of EAs make them appropriate for multi-objective optimization problems (MOPs) [8]. In this work, a newly developed optimization algorithm named multi-objective differential evolution with fuzzy inference-based dynamic adaptive mutation factor (MODE-FM) [9] has been used to optimally design a non-linear vehicle suspension system under different road inputs. A concise reviewing on the past works found in the literature on vehicle optimization problems is stated as follows.

In [10], an LQG problem is used to optimally design the active suspension half car model. In [11], sequential unconstrained minimization technique (SUMT) has been applied to model 3-D vehicle suspension model under different road conditions for achieving better ride comfort and road holding capability. Du et al [12] used linear matrix inequalities (LMI) and genetic algorithms to model non-fragile output feedback H_∞ for designing active quarter car suspension system. Gao et al [13] utilized Linear quadratic (LQ) to optimized hydro-pneumatic active suspension for a non-linear quarter-car model. In [14], a two-degrees-of-freedom linear suspension model subjected to random road profile has been analyzed and optimized based on the Fritz John necessary condition for unconstrained Pareto optimality. By using the Strength Pareto Evolutionary Algorithm in [15], a Pareto-based multi-objective optimization has been done on passive or semi-active suspension system quarter-car models. In [16], a robust Pareto design based on NSGA Ⅱ [17] has been applied to reach a trade-off between ride comfort and road holding ability for a passive linear quarter car suspension. In [8], Pareto optimal design of a five-degree of freedom vehicle vibration passive suspension system has been done by applying a multi-objective uniform-diversity genetic algorithm (MUGA) using a diversity preserving mechanism called the ε-elimination algorithm. The compromise between road holding capability and ride comfort has been accomplished by achieving trade-offs amongst the conflicting objective functions. Crews et al. [18] applied a multi-objective genetic algorithm (MOGA) to optimally design a semi-active quarter car suspension system using skyhook control, feedback linearization, and sliding mode control to achieve good ride comfort and thermal performance. In [19], an active half car model has been adopted to be optimally design by MUGA. Trade-offs are accomplished amongst different Pareto frontiers for reaching proper road holding ability and ride comfort. Mahmoodabadi et al. [20] proposed a method based on the combination of particle swarm optimization (PSO) with convergence and divergence operators named CDPSO for Pareto optimal design of a two-degree of freedom vehicle model with passive suspension. Jamali et al. [21] applied the combination of MUGA and Monte Carlo simulation (MCS) to find Pareto frontiers in the optimal modeling of an uncertain five-degree of freedom vehicle active suspension system. A trade-off robust optimum point was selected from the view of the all the Pareto fronts resulted from the hybrid of MCS and MUGA methods. In [22] a hybrid method based on the combination of genetic algorithm operators and particle swarm optimization algorithm has been utilized for Pareto optimal design of the vehicle passive suspension system used in [8]. Boonlong [23] applied an improved compressed objective genetic algorithm (COGA-II) with convergence detection to seek Pareto frontiers for vibrational model of the five-degree of freedom vehicle model with passive suspension [8]. In [24], a Pareto optimal approach based on the MUGA has been conducted to achieve optimal design of a five-degree of freedom vehicle passive suspension system under random road excitation. In [25], combination of particle swarm optimization and sequential quadratic programming algorithms has been adopted to attain the optimum design model of an eight-degree-of-freedom vehicle vibration system subjected to a random road excitation. In [26], NSGA-II, SPEA2 and PESA-II have been employed for Pareto optimum design of passive half car model under sinusoidal road type profile for achieving good ride comfort and road holding ability. In [27], NSGA-II and Multi-Objective Particle Swarm Optimization-Crowding Distance (MOPSO-CD) algorithm have been implemented for optimization a nonlinear quarter car model including quadratic tire stiffness and cubic stiffness in suspension spring, frame and seat cushion with 4 degrees of freedom considering ride and health parameters. Khalkhali et al. [28] applied NSGA-II combined with MCS for robust Pareto design of suspension model used in [8] with uncertainties under random road irregularities to achieve reliable trade-off between road holding capability and ride comfort. Salehpour et al. [29] presented a methodology based upon DE in conjunction with fuzzy inference system to dynamically tune the mutation factor named Fuzzy Differential Evolution (FDE). This algorithm has been utilized to for single objective optimization of the passive half car model used in [8]. In [30], Pareto optimal design of a product family (NP01 including sedan car, hatchback car, SUV, minivan car and pickup) has been conducted by applying NSGAII, and suggesting the technique for order of preference by similarity to ideal solution (TOPSIS) for achieving

[DOI: 10.22068/ase.2021.595]

the compromise amongst all of the objective functions together. In [31], Pareto design of two degree of freedom nonlinear active vehicle model has been carried out by employing multi-objective differential evolution using fuzzified mutation factor combined with non-dominated sorting algorithm along with crowding distance criterion (MFDE). In this way, sliding mode method in conjunction with skyhook reference model are applied in the vibrational design. In [32], single objective (SOO) and multi-objective (MOO) optimization of half car model with seat-passenger model have been done using genetic algorithm combined with a sorting algorithm ($k-\varepsilon$ optimality method) to achieve trade-off between ride comfort and road holding ability. In [33], Pareto optimal design of half car model used in [8] has been executed by applying MFDE method, presented in [31], for achieving proper performance of aforesaid vehicle under non-stationary random road profile. In [34], regulating of the factors of a nonlinear suspension system was obtained by employing a contrast-based Fruit Fly Optimization Algorithm (c-FOA) on a quarter car model with semi-active suspension using a clipped quadratic parameter varying nonlinear equation. In [35], the approach proposed in [32] is employed for Pareto optimal design of a half car model with semi-active suspension system considering ride comfort and road holding along with extra objectives such dissipated energy and vibration control performance. In [36], PSO has been utilized to optimum design of an active suspension quarter car model by obtaining the optimal gains of the fuzzy adaptive proportional-integral-derivative (PID) controller whose adaptation rules designed by integral sliding surfaces. Jamali et al. [9] presented a multi-objective differential evolution using a fuzzy inference-based dynamic adaptable mutation factor (MODE-FM) for Pareto optimal design of a suspension model used in [8] utilizing a hybrid usage of non-dominated sorting algorithm along with crowding distance criterion. Zhang et al. [37] used an adaptive neural network (NN) optimized control strategy for reaching compromise between ride comfort of passengers and the suspension travel for full vehicle active suspension system with state constraints using backstepping technique and the identifier-actor-critic structure along with Barrier Lyapunov functions.

In this paper, multi-objective DE with dynamically adaptive mutation factor using a combination of non-dominated sorting and crowding-distance criterion (MODE-FM) [9] is employed to optimally design a nonlinear five degree of freedom passive suspension system under different road profiles.

2. Multi-objective Differential Evolution with Fuzzified Mutation (MODE-FM)

A multi-objective optimization problem can be stated as a procedure in which a vector of design variables $X^* = [x_1^*, x_2^*, \dots, x_n^*]^T$ found to attain proper results on:

$$\mathrm{mof}(X) = [f_1(X), f_2(X), \dots, f_k(X)] \quad (1)$$

under such constraints as follows:

a) m inequality constraints

$$g_i(X) \le 0 \qquad i = 1, 2, \dots, m \quad (2)$$

b) p equality constraints:

$$h_j(X) = 0 \qquad j = 1, 2, \dots, p \quad (3)$$

where $X^* \in \mathbb{R}^n$ is the vector of decision variables, and $\mathrm{mof}(X) \in \mathbb{R}^k$ shows the multi-objective values of the associated design variable vector (vector of objective functions), which have to be optimized (minimized or maximized). In addition, concept of Pareto dominance is used in the aforementioned multi-objective optimization [8].

At first, initial population including n individuals (eq. 4) is randomly generated applying uniform distribution, and then the mutation (eq. 5) and crossover (eq. 6) operators are utilized to produce n new individuals called offsprings:

$$x_i^G = \left(x_{1,i}^G, x_{2,i}^G, \dots, x_{d,i}^G\right), \quad i = 1,2, \dots, n \quad (4)$$

In fact, each individual named a target vector (parent vector) (x_i^G) is firstly employed to create a mutant vector (v_i^G) by using a difference vector which indicates direction and length of search process [38]:

$$v_i^G = x_{best}^G + F\left(x_{r_1}^G - x_{r_2}^G\right), \quad r_1 \ne r_2 \ne i \quad (5)$$

Secondly, a so-called trial vector (u_i^G) is made by combining the target and the mutant vector:

$$u_{j,i}^G = \begin{cases} v_{j,i}^G & \text{if } r \le C_r \text{ or } j = J_r, \\ & \qquad j = 1,2, \dots, d \\ x_{j,i}^G & \text{Otherwise.} \end{cases} \quad (6)$$

in which, n, G, d, F, $x_{r_k}^G$ $(k = 1, 2)$, r, C_r and J_r indicate, population size, number of generations, search space dimension, mutation factor, two randomly chosen separate vectors, random number extracted from $[0, 1]$, crossover probability and a

[DOI: 10.22068/ase.2021.595]

parameter to guarantee $u_i^G \neq x_i^G$, respectively. Besides, x_{best}^G will be described later.

As broadly seen in preceding studies, $a = [a_1, a_2, \dots, a_k]$ dominates $b = [b_1, b_2, \dots, b_k]$ (indicated by $a \prec b$), if and only if, $\forall i \in \{1, 2, \dots, k\}$, $a_i \leq b_i \wedge \exists j \in \{1,2, \dots, k\}$, $a_j < b_j$ [8]. Hence, there would be three options as follows:

1. a dominates b, shown by $a \prec b$.
2. b dominates a, shown by $b \prec a$.
3. a and b are non-dominated, shown by $a \asymp b$.

Now, two-step selection of MODE-FM [9] is exerted as follows:

At first step, multi-objective selection operator, or briefly mo-selection (inspired by [39]) is applied based upon the below formula:

$$w_i^G = \begin{cases} u_i^G & \text{if } u_i^G \prec x_i^G, \\ x_i^G & \text{if } x_i^G \prec u_i^G, \\ x_i^G \text{ with } u_i^G & \text{if } u_i^G \asymp x_i^G. \end{cases} \quad (7)$$

It could be readily observed that after using mo-selection, the population count may be in the interval $[n, 2n]$. Consequently, the second step must be applied for tuning the population number to n if necessary and fronting the population. To this end, non-dominated sorting algorithm in conjunction with crowding distance criterion [17] are applied. In this way, firstly, in each generation the individuals of population are arranged based on the notion of Pareto dominance [8], and, accordingly, individuals with no superiority over each others are appointed first order to form first front. Then first front is removed from the population and the procedure is iterated for the remainder of the members of the population to create the other fronts. Secondly, considering each front, a quantity is allocated to each member to unveil the diversity of that in terms of the absolute normalized difference of the objective function evaluation of its two surrounding points. Then the individuals are sorted based upon the aforementioned quantity called crowding distance from the highest to lowest value in each front. As a result, individuals with greater value of crowding distance (belong to the less crowded location) have more hope to join the following generation.

Even though DE is a good, simple and fast algorithm, some flaws can be seen in it. Global exploration ability of DE seems satisfactory, but in contrary, its local exploitation capability is weak at fine-tuning the optimal Pareto front points [40-41]. Further, DE may suffer lack of diversity which happens while the population stagnation or premature convergence occurs. for the sake of conquering the drawbacks of DE mentioned above, fuzzy logic technique is used to dynamically adjust the mutation factor, F, by utilizing two significant parameters as bellows [9]:

1. Generation count
2. Population diversity

It could be easily seen that in the early generations, the algorithm must explore through the feasible region so the quantity of F may better be high for fairly large steps. On the other hand, at the ending levels of the evolution when approaching toward global optimal solution(s), its quantity may better be low for both fine-tuning and hastening the convergence rate. Apart from Generation count, population diversity is the other parameters seems to be effective on the variation of F. As a matter of fact, when the members of population are packed together (low levels of diversity), the low value of F may be proper; in reverse, when the members of population are far from together (high values of diversity), the high value of F may be applicable. Consequently, the mutation factor value is tuned dynamically during searching operation by changing the number of generation and value of population diversity.

As a result, in this work a fuzzy inference system based upon two inputs namely, Generation count and population diversity and one output as mutation factor of type of Mamdani [9] is employed to improve the performance of the differential evolution algorithm. Fuzzy rules used here [9] are presented in Table 1.

Totally, the procedure of modified multi-objective differential evolution using fuzzified mutation factor (MODE-FM) can be expressed as follow [9]:

At first, the process previously mentioned about DE is executed by considering the fact that x_{best}^G is the vector which is randomly selected from the first front of the latest generation heretofore [42] and the mutation factor is adjusted by using the aforesaid fuzzy method including the number of generations and value of diversity. After applying equations 4-7, non-dominated sorting algorithm with crowding-distance criterion is used to form a generation. This process irritates until the stopping criterion will occur. Parenthetically, pseudo code of MODE-FM is shown in Table 2.

[DOI: 10.22068/ase.2021.595]

Table 1: Fuzzy rule-based system used here [9]

Output of fuzzy system is Mutation Factor		Diversity		
		Low	Medium	High
Number of Generation	Low	(…) Very High	(…) High	(…) Medium
	Medium	(…) High	(…) Medium	(…) Low
	High	(…) Very Low	(…) Low	(…) Medium

(…): Mutation Factor must be

3. Multi-objective optimization of nonlinear vehicle vibration model with passive suspension using MODE-FM

Real world engineering models are nonlinear, but for simplicity, in most cases linear models are used instead of nonlinear ones. It is clear that using nonlinearity in models makes the results be more near to real ones. Of course, using nonlinearity in models may result in some complexities and needing more calculating, but as mentioned before the model can be more similar to reality; therefore, in this paper, nonlinear passive vehicle model is utilized for the case of optimization. In addition, nonlinearity in vehicle vibration models can be applied in some ways such as nonlinearity in input [43], in actuator [44] and in suspension model [45]. It is important to notice that in current work, nonlinearity in model has been used.

Multi-objective optimization has been carried out in 2- and 5-objective optimization spaces for the five-degree of freedom vehicle vibration passive suspension system considering nonlinearity under three different road disturbances, namely, double-bump, stationary and non-stationary.

3.1 Nonlinear vehicle vibration model with passive suspension

Half car model with nonlinearity used here is presented in figure 1. Certain parameters of the aforesaid vehicle model have been shown by $\mathrm{m_1} = 40\mathrm{kg}$, $\mathrm{m_2} = 35.5\mathrm{kg}$, $\mathrm{m_c} = 75\mathrm{kg}$, $\mathrm{m_s} = 730\mathrm{kg}$, $\mathrm{I_s} = 1230\mathrm{kg.m^2}$, $\mathrm{k_{p_1}} = 175500\ \mathrm{N/m}$, $\mathrm{k_{p_2}} = 175500\ \mathrm{N/m}$, $\mathrm{l_1} = 1.011\mathrm{m}$ and $\mathrm{l_2} = 1.803\mathrm{m}$ which state forward tire mass, rear tire mass, seat mass, sprung mass, momentum inertia of sprung mass, forward tire stiffness coefficient, rear tire stiffness coefficient, forward and rear suspension position in relation to the center of mass, respectively [8, 22]. Furthermore, thirteen decision variables depicted by $50 \times 10^3 \le k_{ss}\left(\frac{N}{m}\right) \le 150 \times 10^3$ [8, 22], $1 \times 10^3 \le C_{ss}\left(\frac{Ns}{m}\right) \le 4 \times 10^3$ [8, 22], $10 \times 10^3 \le k_{f_1},\ k_{r_1}, \left(N/m\right) \le 20 \times 10^3$ [45], $-100 \times 10^3 \le k_{f_2}, k_{r_2}, \left(N/m^2\right) \le -50 \times 10^3$ [45], $2 \times 10^6 \le k_{f_3}, k_{r_3}\left(N/m^3\right) \le 5 \times 10^6$ [45], $0.5 \times 10^3 \le C_{f_1}, C_{r_1}\left(Ns/m\right) \le 2 \times 10^3$ [45], $0.1 \times 10^3 \le C_{f_2}, C_{r_2}\left(Ns/m^2\right) \le 1.5 \times 10^3$ [45] and $0 < r\,(m) < 0.5$ [8, 22] that express seat stiffness coefficient, seat damping coefficient, nonlinear stiffness coefficients for vehicle suspension $\left(\mathrm{k_{f_i}}, \mathrm{k_{r_i}}, \mathrm{i} = 1, 2, 3\right)$, nonlinear damping coefficients for vehicle suspension $\left(C_{f_i},\ C_{r_i}, i = 1, 2\right)$ and seat position in relation to the center of mass, respectively.

[DOI: 10.22068/ase.2021.595]

Table 2: Pseudo code of MODE-FM [9]

MODE-FM algorithm pseudo code

Input:
n: Number of population
D: Search space of design variables
Iter: Maximum number of generations
$f_j, j = \{1, 2, \dots, k\}$: Objective function
Initializing
g← 0
P^g ← Randomly generating n individuals using D
$f_j(P^g), j = \{1, 2, \dots, k\}$ ← Evaluating fitness of each individual of population
Fronted population ← Applying non- dominated sorting algorithm on population
x_{best} ← Randomly selected individual from first front
Main procedure
While $g \leq Iter$
Div ← Evaluating the population diversity (in decision space)
Fuzzified mutation factor ← Evaluating the value of mutation factor based on the fuzzy inference system data table using g and div
for i ← 1 to n
x ← $P^g(i)$
[a, b] ← Randomly selected $[P^g(r_1), P^g(r_2)] \neq$ x
v: Mutated vector ← Applying mutation operator using fuzzified mutation factor on x_{best} and [a, b]
u: Applying crossover on v and x
w: Applying mo-selection on u and x
$Q^g \leftarrow$ w
$f_j(u), j = \{1, 2, \dots, k\} \leftarrow$ Evaluating the fitness of w
end for
P^g ← Applying non- dominated sorting algorithm with crowding distance criterion on combining P^g and Q^g
x_{best} ← Randomly selected individual from first front
g ← g+1
end while

Equation of motions of the aforementioned vehicle model assuming small angle θ can be presented as follows:

$$z_{ps} = z_s - r\theta \quad (8)$$

$$z_{s_1} = z_s - l_1\theta \quad (9)$$

$$z_{s_2} = z_s + l_2\theta \quad (10)$$

$$F_{ss} = k_{ss}(z_c - z_{ps}) + c_{ss}(\dot{z}_c - \dot{z}_{ps}) \quad (11)$$

$$f_{s_1} = k_{f_1}\left(z_{s_1} - z_1\right) + k_{f_2}\left(z_{s_1} - z_1\right)^2 + k_{f_3}\left(z_{s_1} - z_1\right)^3 \quad (12)$$

$$f_{d_1} = c_{f_1}\left(\dot{z}_{s_1} - \dot{z}_1\right) + c_{f_2}\left(\dot{z}_{s_1} - \dot{z}_1\right)^2 \quad (13)$$

$$F_{s_1} = f_{s_1} + f_{d_1} \quad (14)$$

$$f_{s_2} = k_{r_1}\left(z_{s_2} - z_2\right) + k_{r_2}\left(z_{s_2} - z_2\right)^2 + k_{r_3}\left(z_{s_2} - z_2\right)^3 \quad (15)$$

$$f_{d_2} = c_{r_1}\left(\dot{z}_{s_2} - \dot{z}_2\right) + c_{r_2}\left(\dot{z}_{s_2} - \dot{z}_2\right)^2 \quad (16)$$

$$F_{s_2} = f_{s_2} + f_{d_2} \quad (17)$$

$$m_c\ddot{z}_c = -F_{ss} \quad (18)$$

$$m_s\ddot{z}_s = -F_{s_1} - F_{s_2} + F_{ss} \quad (19)$$

$$I_s\ddot{\theta} = l_1F_{s_1} - l_2F_{s_2} - rF_{ss} \quad (20)$$

$$m_1\ddot{z}_1 = F_{s_1} - k_{p_1}(z_1 - z_{p_1}) \quad (21)$$

$$m_2\ddot{z}_2 = F_{s_2} - k_{p_2}(z_2 - z_{p_2}) \quad (22)$$

in which z_c, z_s, z_i $(i = 1, 2)$, z_{s_i} $(i = 1, 2)$ and θ depict vertical seat displacement, vertical displacement of the center of gravity of the sprung mass, vertical displacement of the unsprung masses, vertical displacement of the ends of the sprung mass and rotating motion (pitching motion) of sprung mass, respectively. It should be noted that indices 1 and 2 describes the axes of forward and rear tires, respectively. Five objective functions are selected as vertical seat acceleration ($\ddot{z}_c$ ($\frac{m}{s^2}$)), vertical velocity of forward tire ($\dot{z}_1$ ($\frac{m}{s}$)), vertical velocity of rear tire ($\dot{z}_2$ ($\frac{m}{s}$)), relative displacement between sprung mass and forward tire (d_1(m)) and relative displacement between sprung mass and rear tire ($d_2(m)$) to be minimized by optimal finding the aforementioned design variables in the multi-objective optimization process. It is supposed that rear tire

[DOI: 10.22068/ase.2021.595]

follows the same path of forward one in each of the road inputs [8].

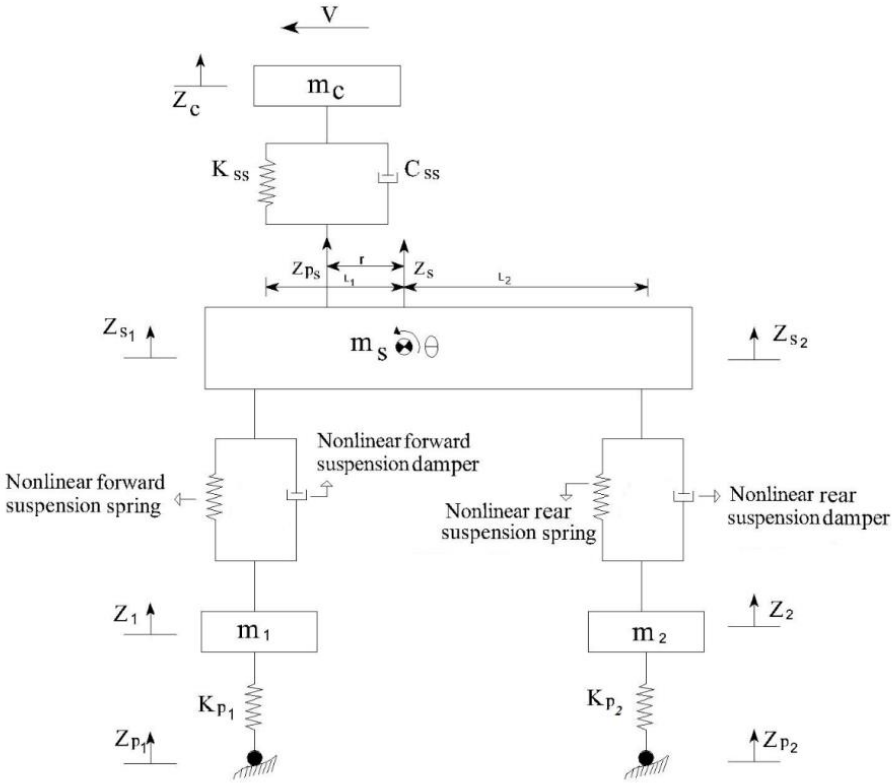

Figure 1: Nonlinear five-degree of freedom vehicle vibration model with passive suspension

As discussed earlier, ride comfort and road holding capability are two major criteria in the suspension design with conflicting nature; as a result, achieving a proper compromise between them has always been a necessary issue. To this end, in this study, $\ddot{z}_c$ represents ride comfort and the other four objectives show road holding ability [9]. Thus, four bi-objective optimizations out of ten possible ones as $(\ddot{z}_c,\ \dot{z}_1)$, $(\ddot{z}_c,\ \dot{z}_2)$, $(\ddot{z}_c, d_1)$ and $(\ddot{z}_c, d_2)$ [8-9, 22] have been firstly carried out to achieve some trade-offs amongst these conflicting criteria, and then, all objective functions are applied in a 5-objective optimization simultaneously.

It is important to notice that there is no notional differentiation between 2- and 5-objective optimization. But, by executing a 5-objective optimization, simultaneously, the results of four different bi-objective processes can be obtained. On the other hand, the Pareto fronts resulted by each bi-objective optimization processes constitute the boundary of left lowest side of each related five-objective planes to verify the authenticity of the optimization procedure.

In case of bi-objective optimization by MODE-FM, a population of 80 members with a crossover probability of 0.9 and the fuzzified adjustable mutation factor has been used for 240 generations for each four optimization processes under three different road inputs. In all four Pareto frontiers, it can be readily observed that obtaining a better value of one objective would normally cause a worse value of another objective.

In case of 5-objective optimization, an optimization consisting of five aforesaid objectives simultaneously, instead of four disparate bi-objective optimizations has been done by applying MODE-FM. The aforesaid five objective functions are used to be minimized concomitantly under three different road excitations. It is worth mentioning that such five-objective optimization can include the results of four bi-objective optimizations. This optimization process is performed utilizing a population size of 80 and for a maximum number of generations of 240 with a crossover probability of 0.9 and the fuzzified adjustable mutation factor.

3.2 Multi-objective optimization of nonlinear model subjected to double-bump excitation

In this subsection, the results of 2- and 5-objective optimization of vehicle model under double-bump excitation (figure 2) [8-9, 22] are presented through figures 3-6. In this part, the vehicle passes the aforementioned disturbance with the constant speed $v = 20\ {}^{m}/_{s}$.

[DOI: 10.22068/ase.2021.595]

As can been easily seen through the aforesaid figures, 5-objective results subsume bi-objective ones, and on the other side of the coin, bi-objective results constitute the border of 5-objective ones, which this significant point prove the correctness of the results of this work.

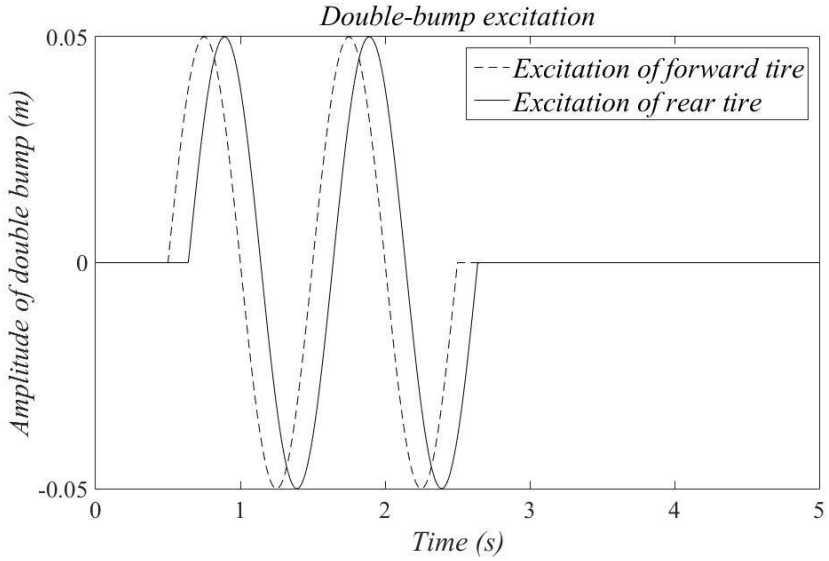

Figure 2: Double-bump input [8-9, 22]

As previously described, whole results attained here are non-dominant and are capable of being utilized by the designer. But, selecting a trade-off optimum point for showing a proper compromise amongst all the aforesaid five objectives is necessary. To this end, all of the quantities resulted by the evaluating of five objectives of each point are mapped into the interval zero to one. Afterwards, the obtained values for each point are summed together. The solution with minimum amount of such summation can be the trade-off point named F_1 here. It can be readily observed that the aforementioned trade-off solution is close to the boundary of the Pareto frontiers in figures 3-6. The values of objective functions and their corresponding decision variables of point F_1 are depicted in Tables 3-4. It is obviously inferred from the results of this work that the significant presented data would not have been obtained without the multi-objective methodology of this paper.

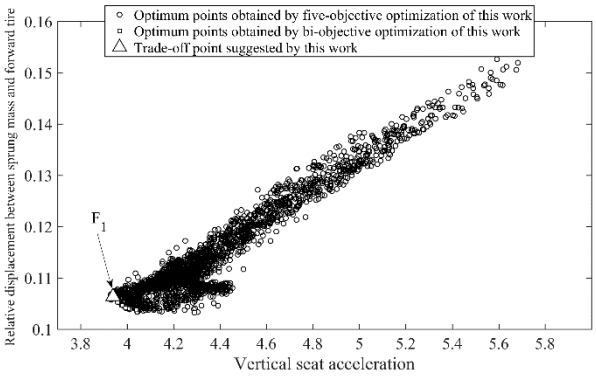

Figure 3: Vertical seat acceleration with relative displacement between sprung mass and forward tire in both 2- and 5- objective optimizations obtained by this work for double-bump input

[DOI: 10.22068/ase.2021.595]

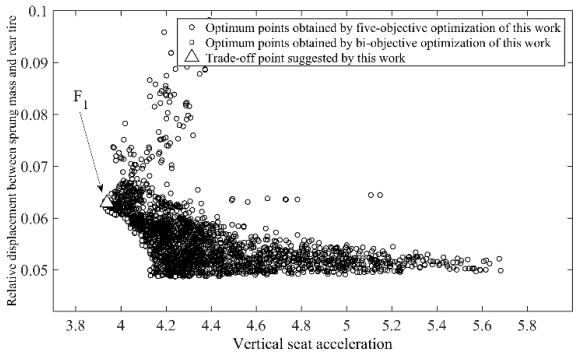

Figure 4: Vertical seat acceleration with relative displacement between sprung mass and rear tire in both 2- and 5- objective optimizations obtained by this work for double-bump input

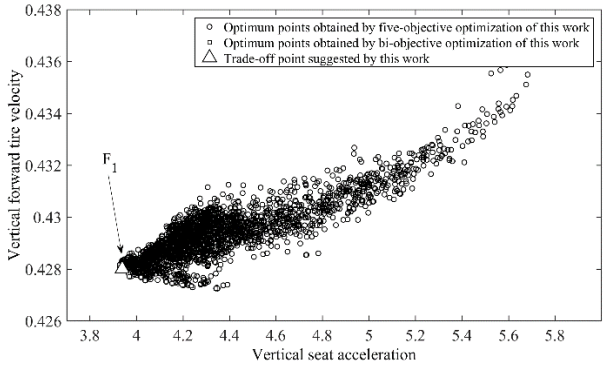

Figure 5: Vertical seat acceleration with vertical forward tire velocity in both 2- and 5- objective optimizations obtained by this work for double-bump input

3.3 Multi-objective optimization of nonlinear model subjected to stationary road excitation

In this subsection, the results of 2- and 5-objective optimization of vehicle model excited by stationary road profile are shown in figures 7-10. Further, the random stationary road surface acts upon the subsequent stochastic differential equation (SDE) [46] which is applied to forward and rear tires:

$$\dot{z}_r(t) + 2\pi\, n_c v\, z_r(t) = 2\pi\, n_0 \sqrt{S_q(n_0)v}\, W(t) \quad (23)$$

where, $n_c = 0.01\, m^{-1}$, $n_0 = 0.1\, m^{-1}$, $S_q = 256 \times 10^{-6}\, m^3$ and $W(t)$ are, namely, road spatial cut-off frequency, standard spatial frequency, coefficient of road roughness for C-level road condition and stationary white noise, respectively [46]. Besides, the nonlinear vehicle model moves through the disturbance with constant velocity $v = 20\ {}^{m}/_{s}$.

It is very obvious in the figures of this part that the results of 5-objective include bi-objective ones, and of course, bi-objective results form the boundary of 5-objective ones, which this important matter confirms the c of the results of this work. The trade-off point for this subsection named F_2 which is obtained by the method described before is shown in the aforementioned figures and is clearly near to the boundary of Pareto frontiers in figures 7 and 9-10. The numerical quantities of objective functions and their related design variables of point F_2 are presented in Tables 5-6.

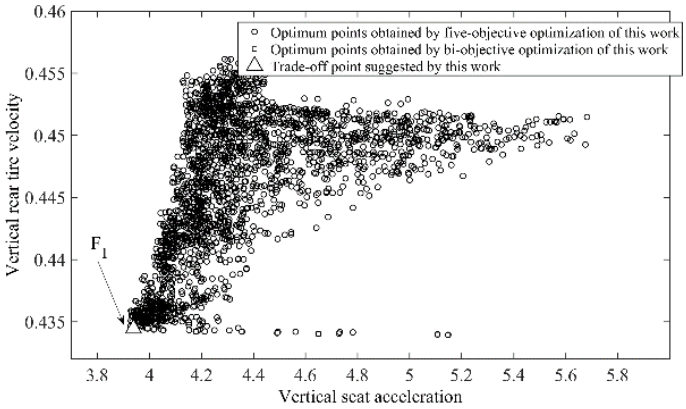

Figure 6: Vertical seat acceleration with vertical rear tire velocity in both 2- and 5- objective optimizations obtained by this work for double-bump input

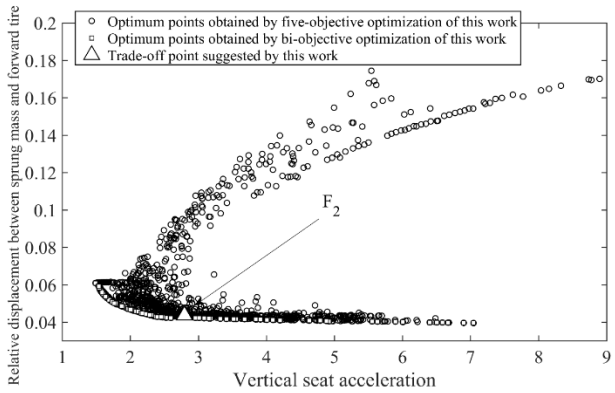

Figure 7: Vertical seat acceleration with relative displacement between sprung mass and forward tire in both 2- and 5- objective optimizations obtained by this work for stationary road input

[DOI: 10.22068/ase.2021.595]

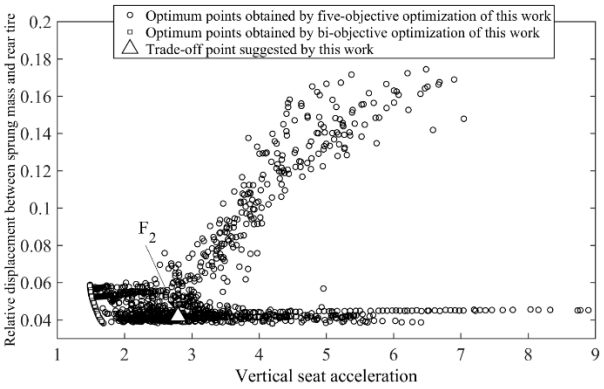

Figure 8: Vertical seat acceleration with relative displacement between sprung mass and rear tire in both 2- and 5- objective optimizations obtained by this work for stationary road input

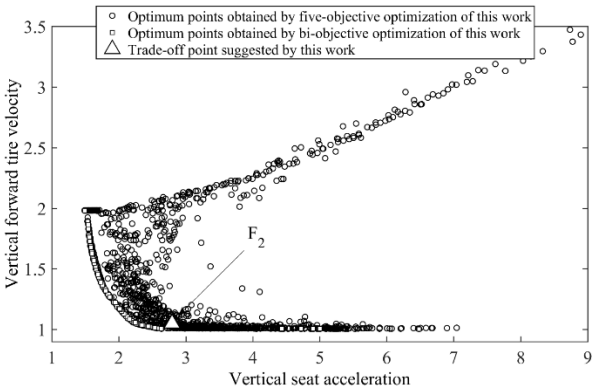

Figure 9: Vertical seat acceleration with vertical forward tire velocity in both 2- and 5- objective optimizations obtained by this work for stationary road input

Table 3: The values of design variables of point F_1designed for double-bump

	k_{ss}	c_{ss}	k_{f_1}	k_{f_2}	k_{f_3}	c_{f_1}	c_{f_2}	k_{r_1}	k_{r_2}	k_{r_3}	c_{r_1}	c_{r_2}	r
F_1	105071.7	3799.241	10004.27	-98311.6	2000288	1999.668	497.9998	10007.02	-98079.2	2014837	1996.526	597.1432	0.46817

Table 4: The values of objective functions of point F_1designed for double-bump

	$\ddot{z}_c$	d_1	d_2	$\dot{z}_1$	$\dot{z}_2$
F_1	3.939229	0.106374	0.062943	0.428003	0.434443

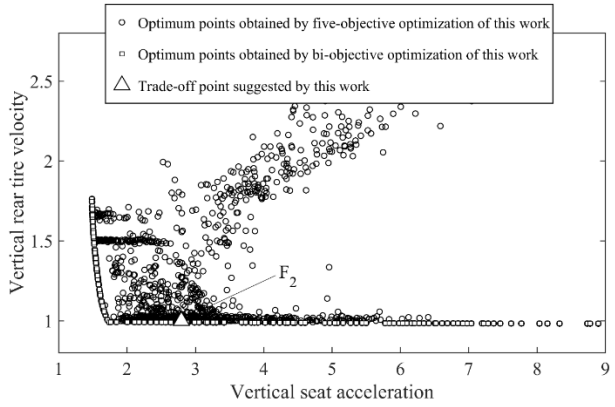

Figure 10: Vertical seat acceleration with vertical rear tire velocity in both 2- and 5- objective optimizations obtained by this work for stationary road input

For the purpose of examining capability of the suggested trade-off points, F_1 and F_2, the vehicle models resulted of their properties are affected by 1000 different stationary roads with constant velocity $v = 20\ ^{m}/_{s}$ to be elaborately observed here (figures 11-15). Collation of the values of the minima and maxima of each of the objective functions per each road input shows the ascendancy of point F_2 in relation to F_1. As a matter of fact, it could be easily observed through the aforesaid figures that the quantities corresponded to the minima and maxima of point F_2 are lower than the related ones of point F_1. In order to achieve better comparison, mean and standard deviation values of each of the objective functions relating to aforementioned trade-off points are depicted in Table 7. The total investigation based on the figures and Table 7 unveils that the vehicle model based on the point F_2 is a more reliable design.

As far as point F_2 is designed for constant speed $v = 20\ ^{m}/_{s}$ for stationary road, it is necessary to inspect the ability of this design confronting with different stationary roads with different velocities. To do so, performance of this point for 1000 different roads with different speeds in interval $15\ ^{m}/_{s}$ to $25\ ^{m}/_{s}$ is compared with performance of that with constant speed $v = 20\ ^{m}/_{s}$ through figures 16-20 and Table 8. Such comparison easily

[DOI: 10.22068/ase.2021.595]

proves that the aforesaid point really has a reliable behavior for different stationary roads with different velocities.

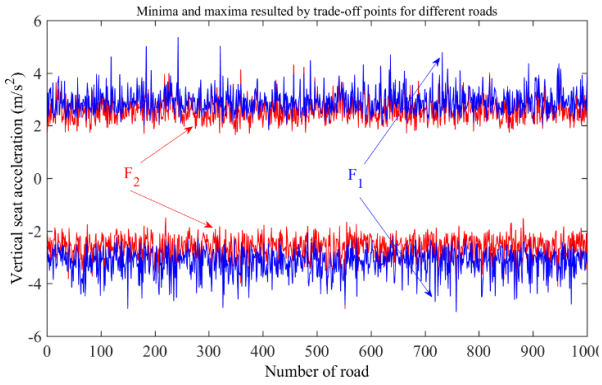

Figure 11: Minimum and maximum points of vertical seat acceleration resulted by points F_1 and F_2 subjected to 1000 different stationary roads

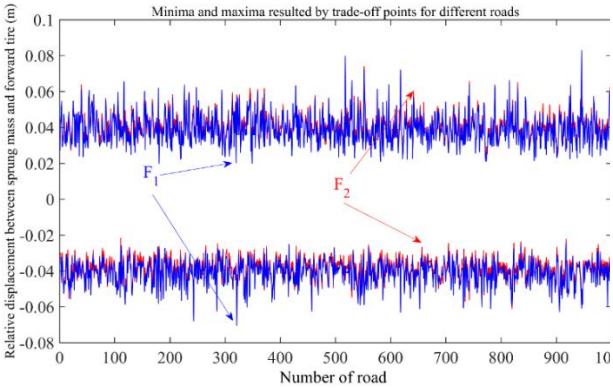

Figure 12: Minimum and maximum points of relative displacement between sprung mass and forward tire resulted by points F_1 and F_2 subjected to 1000 different stationary roads

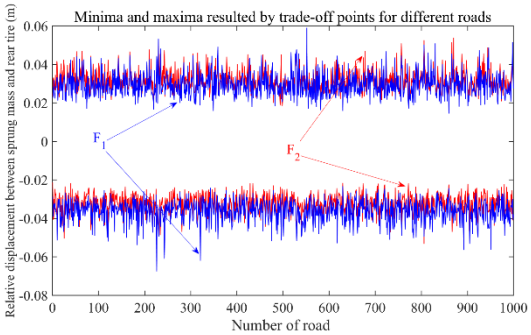

Figure 13: Minimum and maximum points of relative displacement between sprung mass and rear tire resulted by points F_1 and F_2 subjected to 1000 different stationary roads

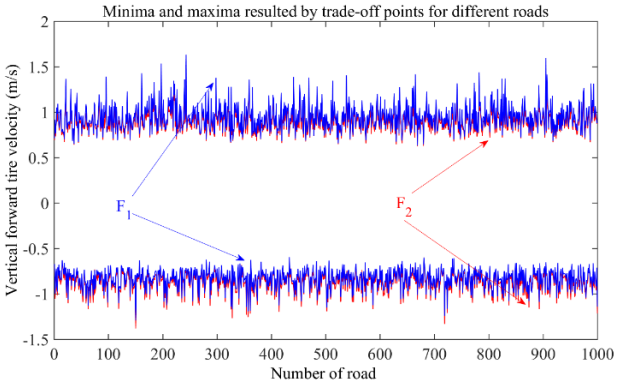

Figure 14: Minimum and maximum points of vertical forward tire velocity resulted by points F_1 and F_2 subjected to 1000 different stationary roads

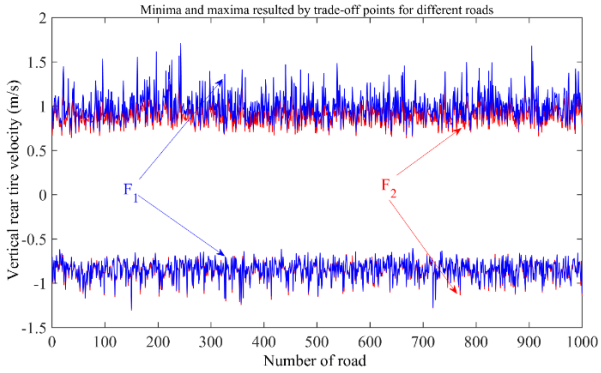

Figure 15: Minimum and maximum points of vertical rear tire velocity resulted by points F_1 and F_2 subjected to 1000 different stationary roads

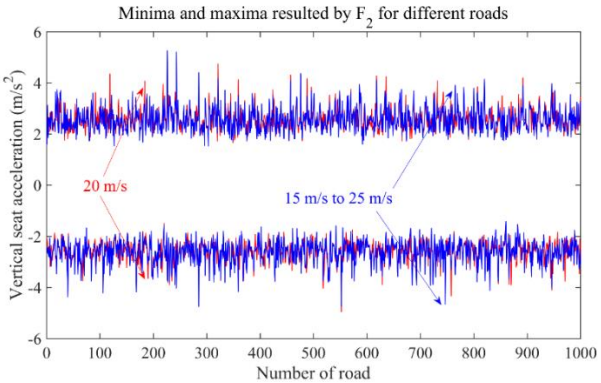

Figure 16: Comparison of values of minimum and maximum points of vertical seat acceleration resulted by points F_2 subjected to 1000 different stationary roads with different velocities from 15 $^{m}/_{s}$ to 25 $^{m}/_{s}$ with 1000 different stationary roads with constant velocity 20 $^{m}/_{s}$

[DOI: 10.22068/ase.2021.595]

Table 5: The values of design variables of point F_2 designed for stationary road input

	k_{ss}	c_{ss}	k_{f_1}	k_{f_2}	k_{f_3}	c_{f_1}	c_{f_2}	k_{r_1}	k_{r_2}	k_{r_3}	c_{r_1}	c_{r_2}	r
F_2	52066.14	1577.224	11271.45	-68385.3	2786702	1954.47	162.1149	19282.17	-71035.8	4242973	1995.564	266.9221	0.256547

Table 6: The values of objective functions of point F_2 designed for stationary road input

	$\ddot{z}_c$	d_1	d_2	$\dot{z}_1$	$\dot{z}_2$
F_2	2.793886	0.043635	0.041861	1.050498	0.999139

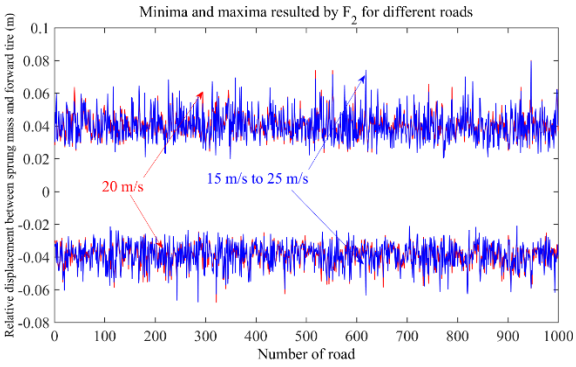

Figure 17: Comparison of values of minimum and maximum points of relative displacement between sprung mass and forward tire resulted by points F_2 subjected to 1000 different stationary roads with different velocities from 15 $^{m}/_{s}$ to 25 $^{m}/_{s}$ with 1000 different stationary roads with constant velocity 20 $^{m}/_{s}$

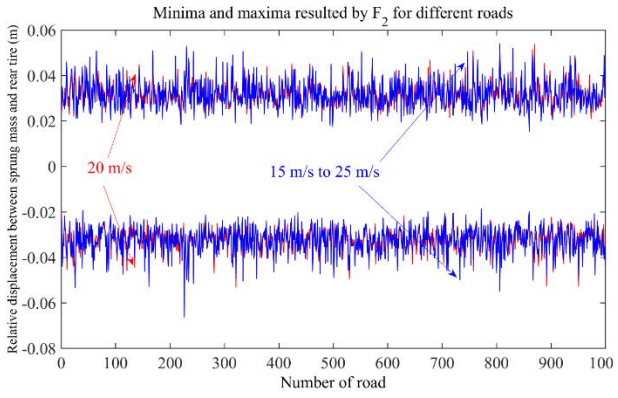

Figure 18: Comparison of values of minimum and maximum points of relative displacement between sprung mass and rear tire resulted by points F_2 subjected to 1000 different stationary roads with different velocities from 15 $^{m}/_{s}$ to 25 $^{m}/_{s}$ with 1000 different stationary roads with constant velocity 20 $^{m}/_{s}$

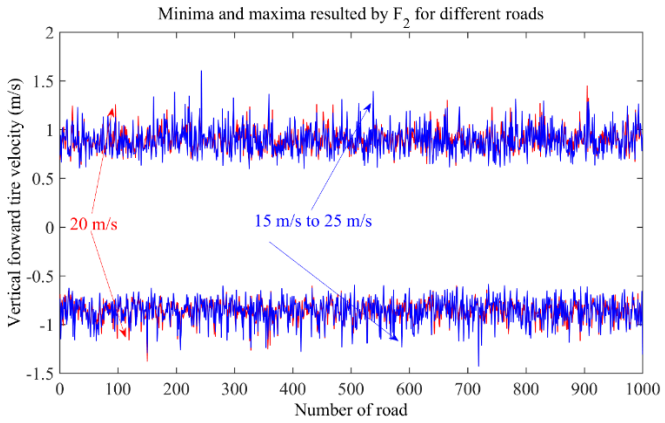

Figure 19: Comparison of values of minimum and maximum points of vertical forward tire velocity resulted by points F_2 subjected to 1000 different stationary roads with different velocities from 15 $^{m}/_{s}$ to 25 $^{m}/_{s}$ with 1000 different stationary roads with constant velocity 20 $^{m}/_{s}$

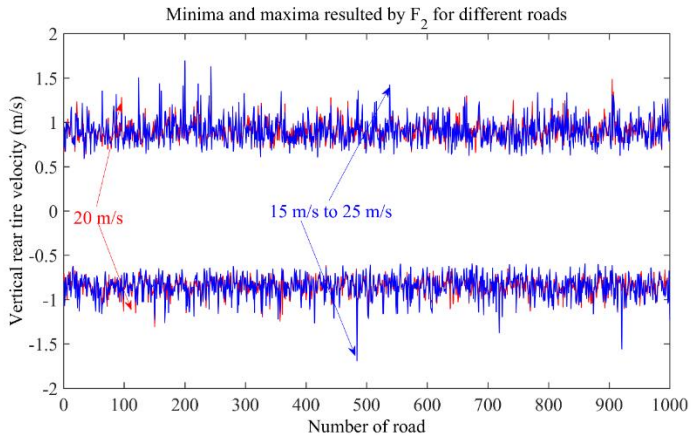

Figure 20: Comparison of values of minimum and maximum points of vertical rear tire velocity resulted by points F_2 subjected to 1000 different stationary roads with different velocities from 15 $^{m}/_{s}$ to 25 $^{m}/_{s}$ with 1000 different stationary roads with constant

[DOI: 10.22068/ase.2021.595]

Table 7: Comparison of mean and standard deviation (Std.) values of each of the objective functions for points F_1 and F_2 for1000 different stationary roads

----------	Mean of $\ddot{z}_c$	Mean of d_1	Mean of d_2	Mean of $\dot{z}_1$	Mean of $\dot{z}_2$
F_1	4.22021	0.06407	0.050287	1.168501	1.165181
F_2	3.709512	0.063625	0.048077	1.171181	1.127168
----------	Std of $\ddot{z}_c$	Std of d_1	Std of d_2	Std of $\dot{z}_1$	Std of $\dot{z}_2$
F_1	0.324672	0.010225	0.005707	0.067804	0.066999
F_2	0.3805	0.010571	0.006086	0.067386	0.062928

Table 8: Comparison of mean and standard deviation (Std.) values of each of the objective functions for points F_2 subjected to 1000 different stationary roads with different velocities from 15 $^{m}/_{s}$ to 25 $^{m}/_{s}$ with 1000 different stationary roads with constant velocity 20 $^{m}/_{s}$

----------	Mean of $\ddot{z}_c$	Mean of d_1	Mean of d_2	Mean of $\dot{z}_1$	Mean of $\dot{z}_2$
20 $^{m}/_{s}$	3.709512	0.063625	0.048077	1.171181	1.127168
15 $^{m}/_{s}$ to 25 $^{m}/_{s}$	3.724094	0.063525	0.047886	1.1709	1.121795
----------	Std of $\ddot{z}_c$	Std of d_1	Std of d_2	Std of $\dot{z}_1$	Std of $\dot{z}_2$
20 $^{m}/_{s}$	0.3805	0.010571	0.006086	0.067386	0.062928
15 $^{m}/_{s}$ to 25 $^{m}/_{s}$	0.433823	0.011434	0.006956	0.106547	0.102852

3.4 Multi-objective optimization of nonlinear model subjected to non-stationary road excitation

Here, the Pareto fronts of 2- and 5-objective optimization results of vehicle model under non-stationary road input are displayed in figures 21-24. Besides, if the nonlinear vehicle model passes through the disturbance with SDE model as equation (23) with changeable velocity, road input will be non-stationary exaction [46]. To this end, $v = v_0 + at$ is applied to (23) with $v_0 = 0$ and $a = 3.6\ ^{m}/_{s^2}$. Other characteristics of formula (23) are based on the points described before.

It can be transparently perceived from the aforesaid figures that the non-dominated optimum points of 5-objective contain the ones of bi-objective, and also, bi-objective results construct the boundary of 5-objective ones, so this significant fact substantiates the exactness of the results of this study. In order to achieve compromise amongst the obtained solutions of this subsection, the so-called trade-off point F_3 is found by the technique described before and shown in the aforementioned figures. Further, it can be easily seen through the figures that this point is rather close to the boundary of the Pareto frontiers. The values of objective functions and their associated design variables of point F_3 are exhibited in Tables 9-10.

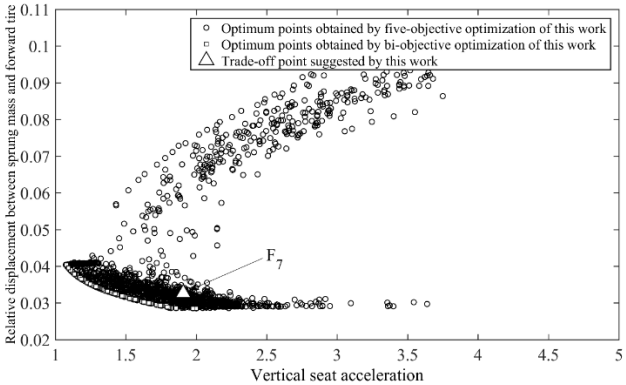

Figure 21: Vertical seat acceleration with relative displacement between sprung mass and forward tire in both 2- and 5- objective optimizations obtained by this work for non-stationary road input

[DOI: 10.22068/ase.2021.595]

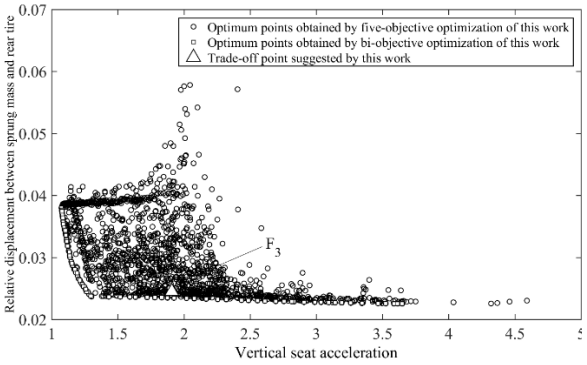

Figure 22: Vertical seat acceleration with relative displacement between sprung mass and rear tire in both 2- and 5- objective optimizations obtained by this work for non-stationary road input

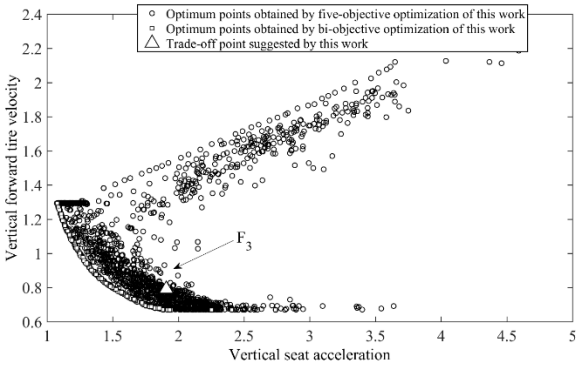

Figure 23: Vertical seat acceleration with vertical forward tire velocity in both 2- and 5- objective optimizations obtained by this work for non-stationary road input

In order to investigate performance of the suggested trade-off point F_3, the vehicle model designed by its properties is affected by 1000 different non-stationary roads using $v = v_0 + at$ with $v_0 = 0$ and $a = 3.6\ {}^{m}/_{s^2}$ and compared with the vehicle model designed by F_2, the point which is suggested as a reliable design by now, under the same non-stationary profile, to be detailly observed here for achieving a final reliable design (figures 25-29). Comparison of the values of the minima and maxima of each of the objective functions based on each road input displays the superiority of point F_3 in relation to F_2. Actually, it is obvious through the aforesaid figures that the values belong to the minima and maxima of point F_3 are rather lower than the corresponding ones of point F_2. For better analyzing, mean and standard deviation quantities of each of the cost functions for aforementioned trade-off points are presented in Table 11. Generally, based on the information extracted from figures and Table 11, the vehicle model based on designed using the characteristics of point F_3 is a reliable solution and can be a final design for different road profiles.

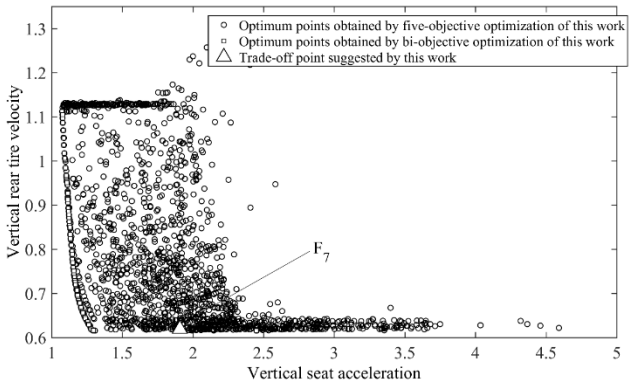

Figure 24: Vertical seat acceleration with vertical rear tire velocity in both 2- and 5- objective optimizations obtained by this work for non-stationary road input

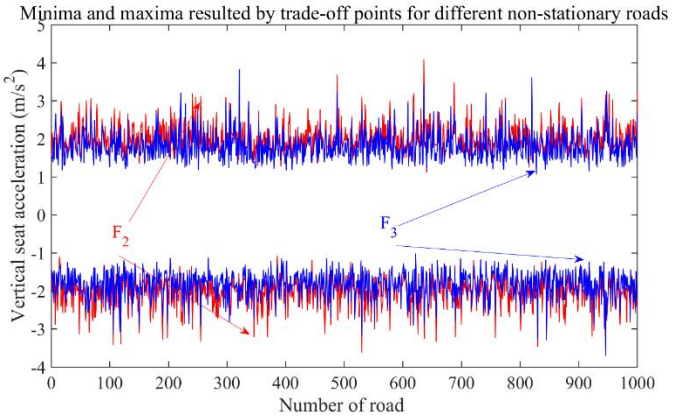

Figure 25: Minimum and maximum points of vertical seat acceleration resulted by points F_2 and F_3 subjected to 1000 different non-stationary roads

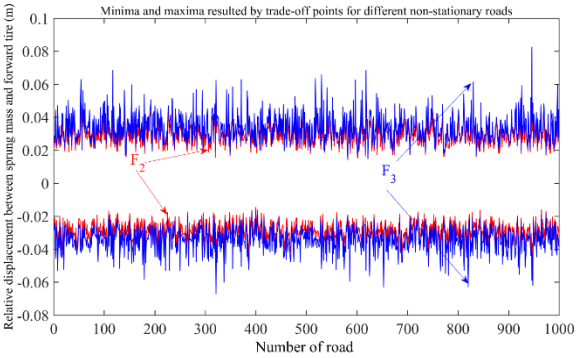

Figure 26: Minimum and maximum points of relative displacement between sprung mass and forward tire resulted by points F_2 and F_3 subjected to 1000 different non-stationary roads

[DOI: 10.22068/ase.2021.595]

Table 9: The values of design variables of point F_3 designed for non-stationary road input

	k_{ss}	c_{ss}	k_{f_1}	k_{f_2}	k_{f_3}	c_{f_1}	c_{f_2}	k_{r_1}	k_{r_2}	k_{r_3}	c_{r_1}	c_{r_2}	r
F_3	51458.64	2730.413	10386.91	-53911	2330358	1434.083	208.7824	19753.46	-73176.1	3454630	1997.571	247.0073	0.460714

Table 10: The values of objective functions of point F_3 designed for non-stationary road input

	$\ddot{z}_c$	d_1	d_2	$\dot{z}_1$	$\dot{z}_2$
F_3	1.90653	0.032672	0.024496	0.791288	0.619554

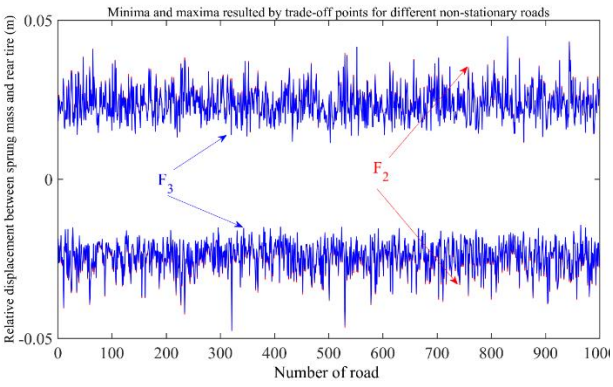

Figure 27: Minimum and maximum points of relative displacement between sprung mass and rear tire resulted by points F_2 and F_3 subjected to 1000 different non-stationary roads

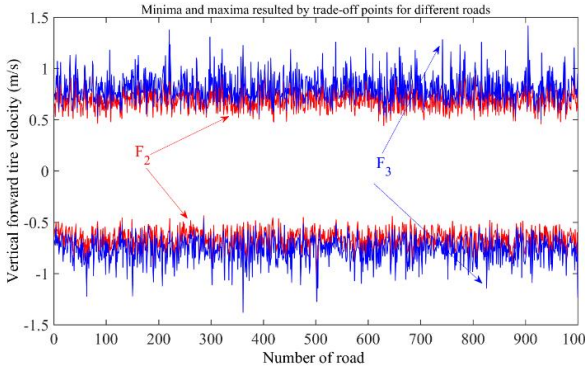

Figure 28: Minimum and maximum points of vertical forward tire velocity resulted by points F_2 and F_3 subjected to 1000 different non-stationary roads

Since F_3 is found based on the optimization of the vehicle model for nonstationary road using $v = v_0 + at$ with $v_0 = 0$ and $a = 3.6\ {}^{m}/_{s^2}$, there is a necessity to investigate its capability under different non-stationary roads with different accelerations. To this end, behavior of the aforesaid point for 1000 different roads with different accelerations varying interval $2.5\ {}^{m}/_{s^2}$ to $4.5\ {}^{m}/_{s^2}$ is achieved to show the contrast with performance of that in acceleration $3.6\ {}^{m}/_{s^2}$ through figures 30-34 and Table 12. The reliable performance of the aforementioned point can be readily observed from the information obtained by different non-stationary roads with different accelerations. The proper behavior of the point F_3 can be also seen for 1000 different stationary roads with different speeds in interval $15\ {}^{m}/_{s}$ to $25\ {}^{m}/_{s}$ comparing with performance of that with constant speed $v = 20\ {}^{m}/_{s}$ in Table 13.

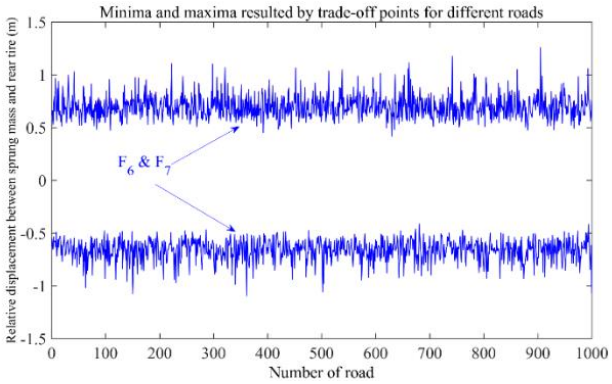

Figure 29: Minimum and maximum points of vertical rear tire velocity resulted by points F_2 and F_3 subjected to 1000 different non-stationary roads

[DOI: 10.22068/ase.2021.595]

Table 11: Comparison of mean and standard deviation (Std.) values of each of the objective functions for points F_2 and F_3 for1000 different non-stationary roads

----------	Mean of $\ddot{z}_c$	Mean of d_1	Mean of d_2	Mean of $\dot{z}_1$	Mean of $\dot{z}_2$
F_2	2.341531	0.038835	0.027547	0.742325	0.668811
F_3	2.038712	0.044947	0.027299	0.857474	0.667705
----------	Std of $\ddot{z}_c$	Std of d_1	Std of d_2	Std of $\dot{z}_1$	Std of $\dot{z}_2$
F_2	0.237652	0.00645	0.003857	0.044723	0.041334
F_3	0.203433	0.008369	0.003777	0.055858	0.041254

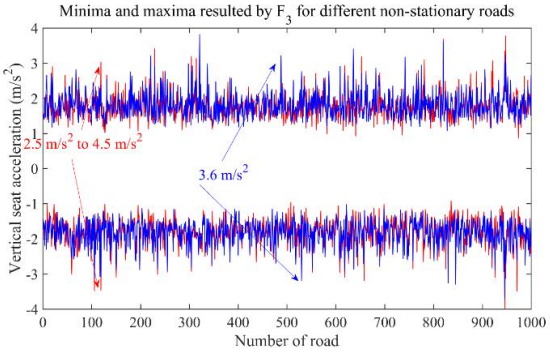

Figure 30: Comparison of values of minimum and maximum points of vertical seat acceleration resulted by points F_3 subjected to 1000 different non-stationary roads with different accelerations from 2.5 $^{m}/_{s^2}$ to 4.5 $^{m}/_{s^2}$ with 1000 different non-stationary roads with constant acceleration 3.6 $^{m}/_{s^2}$

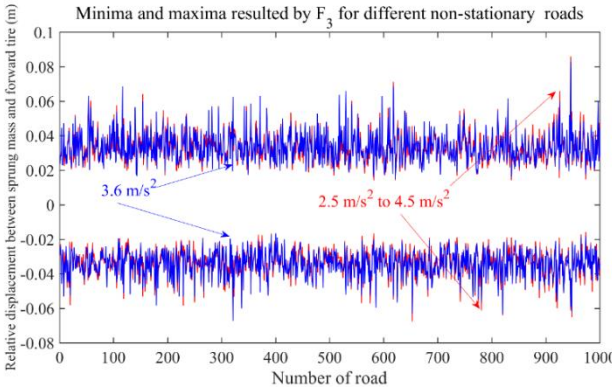

Figure 31: Comparison of values of minimum and maximum points of relative displacement between sprung mass and forward tire resulted by points F_3 subjected to 1000 different non-stationary roads with different accelerations from 2.5 $^{m}/_{s^2}$ to 4.5 $^{m}/_{s^2}$ with 1000 different non-stationary roads with constant acceleration 3.6 $^{m}/_{s^2}$

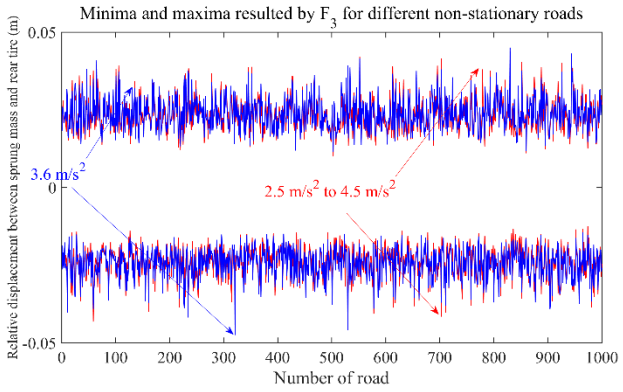

Figure 32: Comparison of values of minimum and maximum points of relative displacement between sprung mass and rear tire resulted by points F_3 subjected to 1000 different non-stationary roads with different accelerations from 2.5 $^{m}/_{s^2}$ to 4.5 $^{m}/_{s^2}$ with 1000 different non-stationary roads with constant acceleration 3.6 $^{m}/_{s^2}$

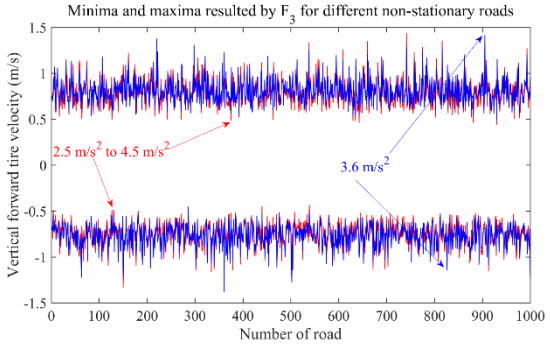

Figure 33: Comparison of values of minimum and maximum points of vertical forward tire velocity resulted by points F_3 subjected to 1000 different non-stationary roads with different accelerations from 2.5 $^{m}/_{s^2}$ to 4.5 $^{m}/_{s^2}$ with 1000 different non-stationary roads with constant acceleration 3.6 $^{m}/_{s^2}$

[DOI: 10.22068/ase.2021.595]

Table 12: Comparison of mean and standard deviation (Std.) values of each of the objective functions for points F_3 subjected to 1000 different non-stationary roads with different accelerations from 2.5 $^{m}/_{s^2}$ to 4.5 $^{m}/_{s^2}$ with 1000 different non-stationary roads with constant acceleration 3.6 $^{m}/_{s^2}$

----------	Mean of $\ddot{z}_c$	Mean of d_1	Mean of d_2	Mean of $\dot{z}_1$	Mean of $\dot{z}_2$
3.6 $^{m}/_{s^2}$	2.038712	0.044947	0.027299	0.857474	0.667705
2.5 $^{m}/_{s^2}$ to 4.5 $^{m}/_{s^2}$	1.995516	0.044007	0.026619	0.840144	0.652071
----------	Std of $\ddot{z}_c$	Std of d_1	Std of d_2	Std of $\dot{z}_1$	Std of $\dot{z}_2$
3.6 $^{m}/_{s^2}$	0.203433	0.008369	0.003777	0.055858	0.041254
2.5 $^{m}/_{s^2}$ to 4.5 $^{m}/_{s^2}$	0.264808	0.009016	0.004495	0.088272	0.073206

Table 13: Comparison of mean and standard deviation (Std.) values of each of the objective functions for points F_3 subjected to 1000 different stationary roads with different velocities from 15 $^{m}/_{s}$ to 25 $^{m}/_{s}$ with 1000 different stationary roads with constant velocity 20 $^{m}/_{s}$

----------	Mean of $\ddot{z}_c$	Mean of d_1	Mean of d_2	Mean of $\dot{z}_1$	Mean of $\dot{z}_2$
20 $^{m}/_{s}$	3.388587	0.074421	0.047103	1.355445	1.125142
15 $^{m}/_{s}$ to 25 $^{m}/_{s}$	3.418297	0.074425	0.046976	1.35577	1.12022
----------	Std of $\ddot{z}_c$	Std of d_1	Std of d_2	Std of $\dot{z}_1$	Std of $\dot{z}_2$
20 $^{m}/_{s}$	0.370063	0.013944	0.005858	0.084173	0.062863
15 $^{m}/_{s}$ to 25 $^{m}/_{s}$	0.479013	0.01513	0.006835	0.126369	0.101926

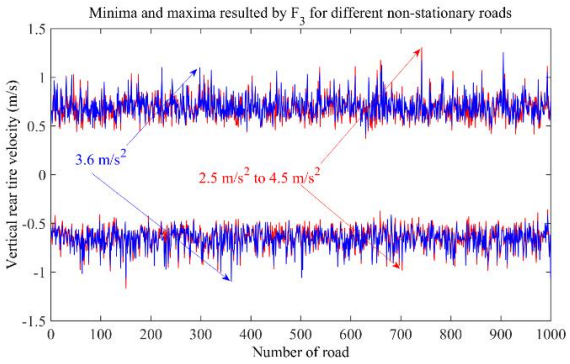

Figure 34: Comparison of values of minimum and maximum points of vertical rear tire velocity resulted by points F_3 subjected to 1000 different non-stationary roads with different accelerations from 2.5 $^{m}/_{s^2}$ to 4.5 $^{m}/_{s^2}$ with 1000 different non-stationary roads with constant acceleration 3.6 $^{m}/_{s^2}$

All things considered, it seems that the vehicle suspension designed based upon the characteristics of point F_3 is a reliable model and can handle road disturbances as good as possible. It should be noted that the precious results obtained here could not have been found without the multi-objective method of this work.

4. Conclusion

A fuzzy multi-objective approach based upon the combination of differential evolution with non-dominated sorting algorithm and crowding distance criterion was successfully used to optimally design of nonlinear vehicle vibration model under different road inputs. The objective functions which conflict with each other were chosen as vertical seat acceleration, vertical forward tire velocity, rear tire velocity, relative displacement between sprung mass and forward tire and relative displacement between sprung mass and rear tire. Three kinds of road excitation applied to vehicle model are, namely, double-bump, stationary random road and non-stationary random road The aforesaid multi-objective optimization of vehicle model help to achieve some significant trade-offs among those objective functions. On the other hand, optimum results of vehicle model subjected to different roads were compared

[DOI: 10.22068/ase.2021.595]

together and it was shown that the design resulted of non-stationary input might be a reliable one. The aforementioned important design of nonlinear vehicle model based on the trade-offs between conflicting objective functions would not have obtained otherwise. Furthermore, it has been depicted that the optimum points attained by 5-objective optimization include those of 2-objective optimization and, therefore, yields more ways for optimal design.

Declaration of Conflicting Interests

The authors declared no potential conflicts of interest with respect to the research, authorship, and/or publication of this article.

Acknowledgements

The authors acknowledge the support provided by Dr. Nader Nariman-zadeh and Dr. Ali Jamali, university of Guilan, Rasht, Iran, for MODE-FM approach utilized in this work.

References

[1] Nurkan Yagiz, Yuksel Hacioglu, Backstepping control of a vehicle with active suspensions, Control Engineering Practice, Vol.16, (2008), pp.1457– 1467.

[2] Shi-An Chen, Jun-ChengWang, MingYao, Young-BaeKim, Improved optimal sliding mode control for a non-linear vehicle active suspension system, Journal of Sound and Vibration, Vol.395, (2017), 1–25.

[3] Michael Fleps-Dezasse, Jonathan Brembeck, LPV control of full-vehicle vertical dynamics using semi-active dampers, IFAC-Papers OnLine, Vol.49, No.11, (2016), pp.432–439.

[4] Jianbo Lu, Mark DePoyster, Multi-objective optimal suspension control to achieve integrated ride and handling performance, IEEE Transactions on control systems technology, Vol.10, No.6, (2002) pp.807-851.

[5] Mohamed Bouazara, Marc J. Richard, An optimization method designed to improve 3-D vehicle comfort and road holding capability through the use of active and semi-active suspensions, European Journal of Mechanics - A/Solids, Vol.20, (2001), pp.509-520.

[6] Huijun Gao, James Lam, Changhong Wang, Multi-objective control of vehicle active suspension systems via load-dependent controllers, Journal of Sound and Vibration, Vol.290, (2006), pp.654–675.

[7] M. Salehpour, A. Jamali, A. Bagheri, N. Nariman-zadeh, Optimum Pareto design of vehicle vibration model excited by non-stationary random road using multi-objective differential evolution algorithm with dynamically adaptable mutation factor, International Journal of Automotive Research, Vol.8, No.4, (2018), pp.2854-2867.

[8] N. Nariman-Zadeh, M.Salehpour, A.Jamali, E.Haghgoo, Pareto optimization of a five-degree of freedom vehicle vibration model using a multi-objective uniform-diversity genetic algorithm (MUGA), Engineering Applications of Artificial Intelligence, Vol.23, (2010), pp.543–551.

[9] A. Jamali, Rammohan Mallipeddi, M. Salehpour, A. Bagheri , Multi-objective differential evolution algorithm with fuzzy inference-based adaptive mutation factor for Pareto optimum design of suspension system, Swarm and Evolutionary Computation, Vol.54, (2020), pp.100666.

[10] R. Krtolica, D. Hrovat, Optimal active suspension control based on a half-car model: an analytical solution, IEEE Transactions on Automatic Control, Vol.37, No.4, (1992), pp.528 – 532.

[11] Mohamed Bouazara, Marc J. Richard, An optimization method designed to improve 3-D vehicle comfort and road holding capability through the use of active and semi-active suspensions, European Journal of Mechanics-A/Solids, Vol.20, (2001), pp.509–520.

[12] Haiping Du, James Lam, Kam Yim Sze, Non-fragile output feedback H_∞ vehicle suspension control using genetic algorithm, Engineering Applications of Artificial Intelligence, Vol.16, (2003), pp.667–680.

[13] B Gao, J Darling, D G Tilley1, R A Williams, A Bean, and J Donahue, Control of a hydropneumatic active suspension based on a non-linear quarter-car model, Proceedings of the Institution of Mechanical Engineers, Part I: Journal of Systems and Control Engineering, Vol.220, No.1, (2006), pp.15-31.

[14] Massimiliano Gobbi, Francesco Levi, Giampiero Mastinu, Multi-objective stochastic optimisation of the suspension system of road

[DOI: 10.22068/ase.2021.595]

vehicles, Journal of Sound and Vibration, Vol.298, (2006), pp.1055–1072.

[15] G. Georgiou, G. Verros, S. Natsiavas, Multi-objective optimization of quarter-car models with a passive or semi-active suspension system, Vehicle System Dynamics, Vol.45, No.1, (2007), pp.77–92.

[16] B. Loyer, L. Jézéquel, Robust design of a passive linear quarter car suspension system using a multi-objective evolutionary algorithm and analytical robustness indexes, Vehicle System Dynamics, Vol.47, No.10, (2009), pp.1253–1270.

[17] K. Deb, A. Pratap, S. Agarwal, T. Meyarivan, A fast and elitist multi-objective genetic algorithm: NSGA Ⅱ, IEEE Transactions on Evolutionary Computation, Vol.6, No.2, (2002), pp.182-197.

[18] John H. Crews, Michael G. Mattson, Gregory D. Buckner, Multi-objective control optimization for semi-active vehicle suspensions, Journal of Sound and Vibration, Vol.330, (2011), pp.5502–5516.

[19] M. Salehpour, A. Jamali,N. Nariman-zadeh, Optimal selection of active suspension parameters using artificial intelligence, International Journal of Automotive Engineering, Vol.1, No.4, (2011), pp.244-255.

[20] M.J. Mahmoodabadi, A. Baghera, N. Nariman-zadeh, A. Jamali, A new optimization algorithm based on a combination of particle swarm optimization, convergence and divergence operators for single-objective and multi-objective problems, Engineering Optimization, Vol.44, No.10, (2012), pp.1167–1186.

[21] A. Jamali, M. Salehpour, N. Nariman-zadeh, Robust Pareto active suspension design for vehicle vibration model with probabilistic uncertain parameters, Multibody System Dynamics, Vol.30, (2013), pp.265–285.

[22] M.J. Mahmoodabadi, A. Adljooy Safaie, A. Bagheri, N. Nariman-zadeh, A novel combination of Particle Swarm Optimization and Genetic Algorithm for Pareto optimal design of a five-degree of freedom vehicle vibration model, Applied Soft Computing, Vol.13, (2013), pp.2577–2591.

[23] Kittipong Boonlong, Multi-objective Optimization of a vehicle vibration model using the improved compressed-objective genetic algorithm with convergence detection, Advances in Mechanical Engineering, Vol.5, (2013), Article ID 131495, 14 pages.

[24] A. Jamali, H. Shams, M. Fasihozaman, Pareto multi-objective optimum design of vehicle-suspension system under random road excitations, Proceedings of the Institution of Mechanical Engineers, Part K: Journal of Multi-body Dynamics, Vol.228, No.3, (2014), pp.282-293.

[25] Luis Roberto Centeno Drehmer, Walter Jesus Paucar Casas, Herbert Martins Gomes, Parameters optimization of a vehicle suspension system using a particle swarm optimization algorithm, Vehicle System Dynamics International Journal of Vehicle Mechanics and Mobility, Vol.53, No.4, (2015), pp.449-474.

[26] Bhargav Gadhvi, Vimal Savsani, Vivek Patel, Multi-Objective Optimization of Vehicle Passive Suspension System using NSGA-II, SPEA2 and PESA-II, Procedia Technology, Vol.23, (2016), pp.361 – 368 (3rd International Conference on Innovations in Automation and Mechatronics Engineering, ICIAME 2016).

[27] Mahesh P. Nagarkar, Gahininath J. Vikhe Patil, Rahul N.Zaware Patil, Optimization of nonlinear quarter car suspension–seat–driver model, Journal of Advanced Research, Vol.7, No.6, (2016), pp.991-1007.

[28] Abolfazl Khalkhali, Morteza Sarmadi, Sina Yousefi, Reliability-based robust multi-objective optimization of a 5-DOF vehicle vibration model subjected to random road profiles, Journal of Central South University, Vol.24, (2017), pp.104–113.

[29] M. Salehpour, A. Jamali, A. Bagheri, N. Nariman-zadeh, A new adaptive differential evolution optimization algorithm based on fuzzy inference system, Engineering Science and Technology, an International Journal, Vol.20, (2017), pp.587–597.

[30] Mohammad Hassan Shojaeefard, Abolfazl Khalkhali, Hamed Faghihian, Masoud Dahmardeh, Optimal platform design using non-dominated sorting genetic algorithm II and technique for order of preference by similarity to ideal solution; application to automotive suspension system, Engineering Optimization, Vol.50, No.3, (2018), pp.471-482.

[DOI: 10.22068/ase.2021.595]

[31] M. Salehpour, A. Jamali, A. Bagheri, N. Nariman-zadeh, Optimum sliding mode controller design based on skyhook model for nonlinear vehicle vibration model, International Journal of Automotive Engineering, Vol.7, Vol.4, (2017), pp.2537-2550.

[32] Georgios Papaioannou, Dimitrios Koulocheris, An approach for minimizing the number of objective functions in the optimization of vehicle suspension systems, Journal of Sound and Vibration, Vol.435, No.24, (2018), pp.149-169.

[33] M. Salehpour, A. Jamali, A. Bagheri, N. Nariman-zadeh, Optimum Pareto design of vehicle vibration model excited by non-stationary random road using multi-objective differential evolution algorithm with dynamically adaptable mutation factor, International Journal of Automotive Research, Vol.8, No.4, (2018), pp.2854-2867.

[34] Stratis Kanarachos, Arash Moradinegade Dizqah, Georgios Chrysakis, Michael E. Fitzpatrick, Optimal design of a quadratic parameter varying vehicle suspension system using contrast-based Fruit Fly Optimization, Applied Soft Computing Volume, Vol.62, (2018), pp.463-477.

[35] Georgios Papaioannou, Dimitrios Koulocheris, Multi-objective optimization of semi-active suspensions using KEMOGA algorithm, Engineering Science and Technology, an International Journal, Vol.22, (2019), pp.1035–1046.

[36] M. J. Mahmoodabadi, N. Nejadkourki, Optimal fuzzy adaptive robust PID control for an active suspension system, Australian Journal of Mechanical Engineering, https://doi.org/10.1080/14484846.2020.1734154.

[37] Jiaxin Zhang,Kewen Li, Yongming Li, Neuro-adaptive optimized control for full active suspension systems with full state constraints, Neurocomputing, Vol.458, (2021), pp.478-489.

[38] R. Mallipeddi, P. N. Suganthan, Q. K. Pan, M. F. Tasgetiren, Differential evolution algorithm with ensemble of parameters and mutation strategies, Applied Soft Computing, Vol.11, No. 2, (2011), pp.1679-1696.

[39] S. Kukkonen and J. Lampinen, DE3: the third evolution step of generalized differential evolution, 2005 IEEE Congress on Evolutionary Computation Available: https://doi.org/10.1109/CEC.2005.1554717.

[40] G. Liu, Y. Li, X. Nie, and H. Zheng, A novel clustering-based differential evolution with 2 multi-parent crossovers for global optimization, Applied Soft Computing, Vol.12, No.2, (2012), pp.663-681.

[41] C. Zhang, J. Chen, and B. Xin, Distributed memetic differential evolution with the synergy of Lamarckian and Baldwinian learning, Applied Soft Computing, Vol.13, No.5, (2013), pp.2947-2959.

[42] I. Gholaminezhad, A. Jamali, A multi-objective differential evolution approach based on ε-elimination uniform-diversity for mechanism design, Structural and Multidisciplinary Optimization, Vol.52, (2015), pp.861-877.

[43] Y. M. Sam, N. M. Suaib, J. H. S. Osman, Proportional integral sliding mode control for the half-car active suspension system with hydraulic actuator, ROCOM'08: Proceedings of the 8th WSEAS International Conference on Robotics, Control and Manufacturing Technology, Hangzhou, China, April 6-8, 2008, 52–57, ISBN: 978-960-6766-51-0.

[44] Lingfei Xiao1 and Yue Zhu, Sliding-mode output feedback control for active suspension with nonlinear actuator dynamics, Journal of Vibration and Control, Vol.21, No.14, (2015), pp.2721-2738.

[45] Vaijayanti S. Deshpande, Pramod D. Shendge, Shrivijay B. Phadke, Active suspension systems for vehicles based on a sliding-mode controller in combination with inertial delay control, Proceedings of the Institution of Mechanical Engineers, Part D: Journal of Automobile Engineering, Vol.227, No.5, (2013), pp.675-690.

[46] Li-Xin Guo, Li-Ping Zhang, Robust H_∞ control of active vehicle suspension under non-stationary running, Journal of Sound and Vibration, Vol.331, (2012), pp.5824–5837.

[DOI: 10.22068/ase.2021.595]